The Effect of variation Longitudinal Ribs Height in Spanwise Direction on Flow and Heat Transfer Characteristics in a Rectangular Duct

Dr. Ekhlas M. Fayyadh
Mechanical Engineering Department, University of Technology/Baghdad
Email: swsw Hassan@yahoo.com
Dr. Moayed R. Hasan
Mechanical Engineering Department, University of Technology/Baghdad
Sahira H. Ibrahim
Mechanical Engineering Department, University of Technology/Baghdad

Received on: 13/6/2013 & Accepted on: 17/12/2015

ABSTRACT

The present work has investigated numerically and experimentally the effect of a streamwise riblet on the flow and heat transfer characteristics for fully developed turbulent flow in a rectangular duct heated with constant heat flux for Reynolds number based on hydraulic diameter range of $(1.5 \times 10^4 - 6 \times 10^4)$.

Numerical simulations have been done by solving the governing equations (Continuity, Reynolds.

Averaging Navier-stokes and Energy) in turbulent regime with appropriate turbulence model Shear-Stress Transport (k-ω) in three dimensions by using the FLUENT version (12.1.2).

The variation of peak to peak height of riblet in spanwise direction ratio with $(h_s/h$ .5)was simulated. The flow structure and heat transfer characteristics (the velocity contours, vorticity contours, secondary flow contours, temperature contours, the distribution of local wall shear stress and heat transfer coefficient in spanwise direction at ribs) were presented as results. Also the effects of ribs on the flow and heat transfer characteristic at duct were presented, as the percentage of average skin friction, Stanton number and the heat transfer efficiency relative to a smooth surface. Experiments were conducted for rectangular duct of aspect ratio =10.

Experimental results indicated an increase in the thickness of hydraulic and thermal sub-layer and shifted up the velocity profile, reducing the skin friction coefficient and Stanton number by about (6 %) and (23%) respectively. The experimental results gave a good agreement with the numerical simulation and previous works.

Keywords: Turbulent flow, drag reduction by Riblet, Heat transfer for ribbed surface

تأثيرتباين الارتفاع للحزوز الطوليه بالاتجاه المستعرض على خصائص الجريان المضطرب وانتقال الحراره داخل مجرى مستطيل

الخلاصه

تناول البحث الحالي دراسة عملية وعدديه لتأثير الحزوز الطولية على خصائص الجريان وانتقال الحرارة للجريان المضطرب المتكامل النمو داخل مجرى مستطيل المقطع مسخن من الاسفل بفيض حراري ثابت لمدى من

https://doi.org/10.30684/etj.2016.112637
2412-0758/University of Technology-Iraq, Baghdad, Iraq

اعداد رينولدزمعتمد على القطر الهيدروليكي يتراوح بين). الدراسة العددية تضمنت حـــــــــل المعادلات الحاكمة (الاستمراية، الزخـــــــم ،الطـــــــاقة) بأستخدام الأنموذج المنـــــــــــــــاسب للحل المتعلق بالجـــــــريان المضطرب(k-ω) Shear-Stress Transport الثلاثي الابعاد بأستخدام البرنامج FLUENT (12.1.2). تضمن الحل العددي دراسةتأثير وتقليل ارتفاع قمه الحزوز المتجاورة بنسبه (h_s/h_L =0.5) للشكل حرف (V) بالاتجاه المستعرض على خصائص الجريان وانتقال الحرارة وتمثلت النتائج العددية بالمخطط الطيفي للسرعة، الدواميه، الجريان الثانوي، درجة الحرارة، اجهاد القص الموضعي، معامل انتقال الحرارة الموضعي) بالاتجاه المستعرض للسطح الاملس والمحزز.كما تم تمثيل النسبه المئوية لمعدل معاملالاحتكاك السطحـــــــــــي وعدد ستانتن. للسطح المحزز وكفاءة انتقال الحرارة نسبه الى الاملس . اجريت الدراسة العملية في مجرى مستطيل ذو نسبه باعيه تساوي(10) . اظهرت النتائج العمليه زيادة في سمك الطبقة اللزجه الطباقية والحرارية للسطوح المحززة وارتفاع في منحني توزيع السرعه ونقصان معامل الاحتكاك السطحي وعدد ستانتن بحوالـــي (6 %) و (23%) .اظهرت النتائج العمليه توافق جيد مع النتائج العدديه والدراسات السابقة.

INTRODUCTION

High efficiency of energy utilization contributes not only to energy saving, but also to improve the environment. A great deal of attention has been given to the design and redesign of aerodynamic and hydrodynamic devices, such as aircrafts, submarines, long-distance cargo ships, and turbine. Viscous drag has been considered one of the major barriers to further optimization of most aerodynamic and hydrodynamic device. Even a small amount of drag increase can have a great economic impact if a large number of units are involved. The rising costs of energy have necessitated new researches directed toward the viscous drag reduction of turbulent boundary layers. Drag reduction has a number of positive effects, namely, reduced fuel consumption with associated economic and environmental consequences. Longitudinal ribs are well known means of passive drag reduction in turbulent boundary layer over flat plate with optimally shaped geometry and when properly adapted to the flow conditions. They are capable of reducing wall shear stress by about 7% **[1]**.

Chen et al. [1] investigated experimentally the possibility of drag reduction for grooved channel with dimensions of (30 mm×30 mm×700 mm) using water as working fluid at range of ($h^+ < 25, and\ s^+ < 100$) .The experiments have been carried out in square water channel. Eleven models will be tested, eight of them are V-groove riblet with different height and spacing for tip angles of (51.3,75.12,98.6,110) degree and at range of Reynolds number (4×10^3- 4×10^4) based on the hydraulic diameter. The results for all riblets models showed that drag reduction is possible if the heights and space are less than (25 and 100), respectively in terms of the law of the wall coordinates. Grooving of flow surface is suggested as being a possible method of passive drag reduction in internal flow.

Djenidi and Antonia [2] developed (k – ε) turbulence model for calculating the skin friction , mean velocity distributions, the Reynolds stress and kinetic energy distributions in a turbulent boundary layer over riblets for low Reynolds. The results are generally in a good agreement with the available experimental data.

Choi et al. [3] investigated experimentally the heat-transfer characteristics of triangular-profiled riblet surfaces by comparing them with those of a smooth surface of an identical construction in a thermal turbulent boundary layer. The experiments were carried out at a low-speed wind tunnel. The results indicated that the heat-transfer coefficient over the riblet surfaces is increased from that of a smooth surface by 10%. This increasing is obtained without incurring the drag penalty usually associated with a modified surface geometry, suggesting that there is an apparent breakdown of the Reynolds analogy over the heated riblet surfaces. The logarithmic temperature profile of the boundary layer over the riblet surface is shifted downward, suggesting that the thickness of the thermal viscous sub layer is reduced.

Lin et. al. [4] investigated experimentally the drag reduction in pipes lined with film of groove equilateral at fully developed turbulent flow through (25.4 mm) and (50.8 mm) diameter pipes using water as working fluid. The maximum drag reduction occurs when the height and space of the riblets are $h^+(11-16)$ and $s^+(11-13)$respectively. It seems excellent agreement with previous investigations for pipe flow and boundary layers. The maximum drag reduction achieved is between (5-7%).

Benhalilou and Kasagi [5] investigated numerically the turbulent heat and momentum transfer characteristics over riblet using a non-linear low-Reynolds number (k-ε) model together with several turbulent scalar flux representations. The results are obtained at fully developed channel flow with triangular riblets. The comparison of the drag variation prediction with previous experimental and numerical data shows that the (k-ε) turbulence model can simulate the turbulent flow over this complex surface reasonably well. Under the drag reducing conditions, possible departure from the Reynolds analogy is investigated at various Reynolds and Prandtl numbers.

It is shown that the skin friction is reduced over the riblet surface; the heat transfer performance can actually be increased beyond that on a smooth wall, although the discrepancy with the experimental data is not negligible.

Stalio and Nobile [6] investigated numerically the flow and heat transfer over riblets at fully developed laminar and turbulent regimes by means of direct numerical simulation. The simulations are performed in a channel with a Reynolds number $\mathrm{Re}_\tau = 180$ based on the wall shear velocity, for a fluid with$\mathrm{Pr} = 0.71$.

Four different ribbed channels are considered under a constant heat flux boundary condition and corresponding to ridge angles$(45°, 60°)$ and riblet spacings$^+(20,40)$. The results indicated that drag and Stanton number over a smaller spacing $s^+ = 20$ ribs decreased by (2%) and (25%) respectively and the drag increasing by (5%) while Stanton number decreased by (11%) over the larger spacing ribs$s^+ = 40$.

In the present work the effect of variation of peak to peak height of riblet in spanwise direction with ratio of $/h$)on the flow and heat transfer at rectangular duct of)will be investigated numerically and experimentally using air as working fluid at Reynolds number range of $(1.5\times10^4 - 6\times10^4)$based on hydraulic diameter.

Numerical Solution

A computational fluid dynamic analysis of three-dimensional rectangular duct model, provided with smooth and ribbed surface as shown in Fig (1).A constant heat flux is applied uniformly on the lower surface of the duct. Different inlet velocities are considered in the range of turbulent regime using air as working fluid .|The thermal properties of fluid are considered in depended on temperature, this computations are performed by using ANSYS FLUENT 12.1.2 Code.

The governing equations of (continuity, momentum, and energy) are solved for steady state, incompressible and Newtonian fluid**.** A segregated method, and a second –order upwind scheme is chosen to solve the governing equations. The SIMPLE Coupling is chosen as scheme to couple pressure and velocity.

1.ContinuityEquation

— ….. (1)

2.Momentum Equation

—(ρ) — —[((— —) - —)] —(−ρú$_i$ú$_j$) ..... (2)

3.Energy Equation

$$—[u_i(\rho E + P)] = \frac{\partial}{}\left[\left(k \quad ——\right)— \quad (\tau_{ij}) \quad\right] \quad \text{.... (3)}$$

Where E is the total energy

– – .... (4)

(τ_{ij}) Is the deviator stress tenser, defined as:

$$(\tau_{ij}) \quad = \mu_{eff}\left[\left(\frac{}{i} + \frac{}{j}\right) - -\delta_{ij}\frac{}{i}\right] \quad \text{... (5)}$$

... (5a)

The transport equations for Shear Stress Transport k-ω model are reported in the forms:

— —(Γ —) ..... (6)

— —(Γ —) .... (7)

The effective diffusivities for the SST k- ω model are given by

— ..... (8)

— .... (9)

Where and are the turbulent Prandtl numbers for k andω, respectively. The turbulent viscosity is computed as follows:

$$\frac{}{_1/\sigma \qquad)/\sigma} \quad \text{.... (10)}$$

$$\frac{}{_1/\sigma \qquad)/\sigma} \quad \text{.... (11)}$$

$$\frac{}{[—]} \text{.... (1.12)}$$

The modelconstants are shown in table.1

Table. 1 Model constants

Geometrical Description

Three dimensional rectangular duct with dimensions of (50 mm, 500 mm, 5250 mm), height, width and length respectively, depicted in Fig.1 .The upper surface and sides are made up from (10 mm) Perspex .The lower wall made up from (10 mm thickness) Aluminum and constant heat flux of (600 W/m^2) has been applied on the bottom wall which provided with equal length (500 mm) smooth and ribbed surface at the fully developed region of the duct. The dimensions of ribbed surface shown in Fig.2.

The incoming flow is at different uniform velocities, corresponding to Reynolds Numbers range from ($1.5 \times 10^4 - 6 \times 10^4$), and at ambient temperature and pressure, no slip condition along the walls and periodic along the duct sides.

Experimental set up and Methodology

Fig. (3) shows the schematic diagram of experiment set up. The experimental facility consists of

1. Test Rig: Rectangular duct of aspect ratio of (W/H) =10 was considered, using air as the working fluid. Air enters the duct through a contraction cone (contraction ratio of (7)) with bell mouth entry of cubic profile of contraction. The bell mouth performs function that provides a smooth undistributed flow into the duct and it contain screen wire and honey combs that provides a smooth and uniform distributed flow into the duct. The duct of (5250 mm) long and (50×500) mmcross - sectional area . It can be divided into three sections. The first section is developed flow section of (3000 mm) long with triple wire at its entrance. The second section is the test section of (1220 mm) and finally the exit section of (1030 mm) long .The lower surface of duct was made from (T-305) aluminum of thickness (10) mm. This layer of aluminum is followed by heaters, which is covered by two layer of Mica .To reduce the thermal losses to ambient; the Mica is covered by fiberglass of (35 mm) and (5 mm) wood layer. The wall surface temperature was measured by (93) K-type thermocouples in (z-x) plane. Thermocouples were inserted in holes drilled from rear face of Aluminum sheet with (2) mm diameter and (9) mm depth. The upper surface of the duct was manufactured from Perspex with (10 mm) thickness. It was drilled from the inner wall with hole of diameter (1 mm) to depth of (4 mm) and then enlarged to (4 mm) diameter to measure the static pressure drop [**8**].

2. Air supply equipment: Air is the working fluid directly supplied into the system by a centrifugal blower. It was driven by A.C motor of 5.5 kW at 2900 rpm. The air velocity at the duct was controlled using a sliding gate sited in the outlet of the blower. The blower was connected to wooden box with dimensions of (700 mm ×700 mm×650 mm) through a flexible circular duct of (400 mm) diameter in order to reduce the vibration and damp any disturbance for air flow stream.

3. Heating system: A plate type heater was used for heating the lower surface of the duct with a uniform surface heat flux (600W/m^2). This heater was manufactured from Mica sheet and electric wire with high resistance. It was consists of (105) Mica strips of (40 mm × 480 mm) dimensions, their power supplied controlled by a (Varic).

4. Ribbed surface and its manufacturing: Aluminum plate with dimensions of (mm)and thickness (10 mm) was used for manufacturing the test section .The CNC was usedto machinethe smooth and ribbed parts with 500mm widthand (500mm) long. The big riblets are of ($s = 1mm, h = 1mm$) and the small riblet is with(s).

5. Measuring system: A traversing mechanism was manufactured for holding the measurement devices to measure the local and bulk temperature and velocity of fluid in three dimensions (x, y, z). Flow mean velocity of air through the duct calculated from integration of the measured velocity profile through the duct. The static pressure tapings were made along the duct and test section, the wall temperature along the lower wall by K-type thermocouples; inlet and exit air temperatures are measured by T-type thermocouples. The current and voltage of the heater are measured by multi-meter. The temperature and velocity distribution are measured by hot wire anemometer and flat pitot tube.

Data Redaction

Percentage of skin friction

———— ....(13)

Percentage of Stanton number

———— ……..(14)

Efficiency of riblet is

————— ..…..(15)

The wall shear stress is calculated as:**-.**

—— …….. (16)

The friction velocity is calculated as**:-**

$= \sqrt{—}$ …….. (17)

The average surface skin friction is calculated as follows**:-**

—— …….. (18)

The average surface heat transfer coefficient is calculated as**:-**

$\bar{h} =$ ————— ……... (19)

1. The average Stanton number *is* calculated as:-

$\frac{\bar{h}}{}$ ——— ……. .(20)

Peutkhov:C … (21)

Mc Adams:

Dittus-Bolte:Nu

…...… (23)

120)

Peutkhov: $Nu = \frac{f/2}{(C_f/2)^{1/2}(\quad^{2/3}\quad 1)}$ ..... (24)

Results and Discussion

A. Numerical Results

1. Local Flow Characteristics (velocity, vorticity and secondary flow) at Riblet

Fig. (4) shows the effect variation of peak to peak riblet height in spanwise direction on the velocity, vorticity and secondary flow contours at Reynolds numbers (1.5×10^4).

As peak to peak height ratio (height of small rib/height of large rib) are decreased from (1 to 0.5), the velocity magnitude is increased and being widely spaced in the large space of valley (distance between larger riblets), this corresponding to higher velocity change over the large peak and in the valley. For changing ribs height ratio to (0.5) the velocity magnitude increased by (6 %) at Reynolds number of (1.5×10^4) , relative to same peaks height model [height ratio=1] in the valley especially at widely spaced of big ribs, this corresponding to higher shear stress. From the vorticity distribution contour, it can be noted that the strength of secondary vortex (induce by the riblet tip effect) will be increased at the tip of larger ribs. The strength of secondary vortex (induced by the large ribs tip) will be increased by (4%), compared to the equal height rib [height ratio=1] and strong secondary flow and cross flow interacts with ribs to produce a secondary flow which is associated with vertical mixing and increased viscous drag...

2. The Local Wall Shear stress

The local wall shear stress distribution in the spanwise direction over the ribbed surface [for the two height ratios (1 and 0.5)] compared to smooth surface at three different Reynolds numbers are illustrated in Fig. (5 A, B).

In general, it can be seen that the skin friction in the valley is less than the skin at a smooth wall, indicating small velocity gradient in the valley. A traverse motion from the riblet peak through the valley up to neighboring peak is important, it is seen near the peaks, the skin friction due to riblet is higher than that for smooth surface wall friction due to strong secondary vortices at the peak of riblet that have mechanism for the transport of high momentum fluid into the valley. When traversing from the peak via the midpoint toward the valley, however, it is found that the friction quite rapidly decreases to a level lower than the average due to the absence of the fluctuation in the riblet valleys, and the turbulent Reynolds number is indeed small there.

The flow field inside the valley is dominated by the viscous force and is dynamically inactive under the drag reducing condition. The flow in the valley is slow and almost laminar, and that turbulence intensities decreased over the valley and increased over the peak, as shown in the Figs. (ٰ).

3.local Heat Characteristics at Riblet *(temperature)*

The temperature contours have been shown in Fig(ٰ) it can be seen temperature magnitude inside the valley is larger than peak, since the turbulent intensity decreases over the valley. There is no much dynamic activity in the riblet valley compared with peak, therefore a small gradient of temperature at the valley is observed as compared to around peak (decreasing heat transfer at valley). There is analogy between the heat and momentum transfer as Reynolds number increased up to $\mathbf{(6 \times 10^4)}$, the flow is more turbulent and the temperature extended more inside the valley and around peak, resulting in increases in heat transfer. As change of height ratio from 1 to 0.5,secondary flow has a higher value ,resulting to transport low temperature fluid away from the solid wall (around the peak) and pushed towards the wall of the valley it is clear when the contour are buckled, This phenomena leads to enhance of heat transfer.

4. The local Heat Transfer Coefficient.

The local heat transfer coefficient distribution in the spanwise direction over the ribbed surface [for the two height ratios (1 and 0.5)] compared to smooth surface at three different Reynolds numbers are illustrated in Fig. (8 A,B).In general, the heat transfer over the riblet peak is larger than in valley due to the secondary vortices at peak that has mechanism for transport the cooled fluid into the driblet valley, these secondary vortices play an important role in heat transfer process (only the riblets peak vicinity contributes to heat transfer). When traversing from the tips via the midpoint to the valley, however, it is found that the heat transfer quite rabidly decreases to a level lower than average of smooth surface due to small value of fluctuation and Reynolds stress.

This is an indication of the fact that the amount of the exchanging heat is the small in the valley; it can be say that the heat transfer mechanism is dominated by conduction in the riblet valley. As Reynolds number increases, the heat transfer also increases.

5. The percentage of Average Skin friction coefficient and Stanton number and heat transfer efficiency.

The percentage of average skin friction coefficient, average Stanton number (relative to smooth surface) and the heat transfer efficiency of three different Reynolds numbers It can be shown in Fig (9 A,B,C) As the height ratio decreased form (1 to 0.5), the ribs will be less effective in drag and heat transfer reduction , as compared to equal height ribs at Reynolds number (1), average skin friction coefficient, average Stanton number(12 %, and 40 %,) , while (16 %, and 42%). At Reynolds number (6×10^4),small variation occurs in the efficiency of ribs for all Reynolds numbers, indicating that the effect of Reynolds number disappeared when the ratio of height was decreased. The results agree well with previous studies which indicated that the maximum viscous drag reduction occurs when (h/s=1) **[4],** they found that for ribbed channels, the heat transfer performance can be increased, beyond that on a smooth wall, only for high Prantdl number fluids. The predicted values of the viscous drag and heat transfer are in a good agreement with **[5].**

5. Experimental Results

1. Local flow and heat transfer characteristics (velocity, temperature)

The flow characteristics, the average skin friction coefficient over ribbed and smooth surface at different Reynolds numbers, can be shown in Fig. (10). It is found that the average wall skin friction can be reduced over the riblet surface approximately around (6) %.

Law of wall: Effect of the riblet on the velocity profile can show in Fig. (11) at Reynolds number of(1.5×10^4). In this figure, the upward shift of velocity profile is over the riblet surface as compared to that over smooth surface, the logarithmic law of the wall for smooth and ribbed surfaces

It can observe that the experimental data for smooth surface gives a good agreement with the Law of wall **[5]**.

The presence of the riblets leads to change the behavior of this law. In other word, the effect of ribbed surface on the velocity profile is to shift the log-law profile upward. This shaft is caused by the adjustment of the balance between the turbulent energy production and the viscous dissipation. This adjustment is reflected by an increase of the viscous sub-layer thickness **[6]**.

The heat transfers by forced convection is calculated from the energy balance in as follows:-

Fig. (11), shows the average Stanton number for smooth and ribbed surface at different Reynolds numbers. It was found that the average Stanton number decreased by the ribbed surface around (23%) for Reynolds number range of$(\mathbf{1.5 \times 10^4 - 6 \times 10^4})$.

Effect of the riblet on the temperature profile can be shown in Fig. (12). In this figure, the upward shift of temperature profile is over the riblet surface as compared to that over smooth surface, indicating the increase of thickness of thermal boundary layer for the riblet surface.

As shown in figure, the temperature measured over smooth surface is fitted to Kader law of temperature **[5]**. It is clear from figure that the temperature profile over the riblet surface is shifted upwards compared with that over the smooth surface at region$y^+ > 30$.

Verification of Present Work

Verification of Experimental Work

Regarding the authenticity for the case of smooth surface of the experimental results (average skin friction and Stanton number), a comparison with literature is carried out to ensure the validity and accuracy of the experimental measurement data. The average skin friction coefficient compared with the empirical equations (1.21) and (1.22) **[6]**.

The average Stanton number is compared with the empirical correlations equations (1.23) and (1.24) **[6].**

It can be seen from Figs. (13 and 14), that there is a deviation between results of present work and literature with around (10 %) for average skin friction coefficient and (7 %) for average Stanton number, which gives a good sign to the accuracy of the results.

Comparison between Experimental and Numerical of present Work

Comparison between the experimental and numerical results[Wall law of velocity, **Kader law** of temperature, the average skin friction coefficient and average Stanton number] for the smooth and ribbed surface in the present work are shown in Figs. (15 and 16). It is found that there is a good agreement with slight discrepancies between the numerical and experimental results. These discrepancies might be partially attributed to the measurement difficulty near the riblets. The maximum deviation in skin friction coefficient and Stanton number was about (11 %) and (13 %), respectively.

CONCLUSIONS

1. The wall shear stress and heat transfer coefficient in the valley are smaller than around the peak since there is no much dynamic activity in valley.
2. Large streamwise vortices formed near the riblet peaks. This induced secondary vortices which play an important role in transfer the cooled fluid from the peak toward the valley.
3. As peak to peak rib heights ratio are changing in spanwise direction from (1) to (0.3), the viscous drag and heat transfer increased. The percentage of reduction in skin friction coefficient and Stanton number decreases, as compared to the height ratio (1) by (12 %, 13%) and (40 %, 30%), respectively at Reynolds number(1.5×10^4), the same tend noted at whole rang Reynolds number Reynolds number$(1.5 \times 10^4 - 6 \times 10^4)$.
4. The near wall velocity profile over the ribbed section was shifted upward compared with smooth surface, which indicated a decreasing in the velocity gradient and increasing the viscous layer thickness at the wall.
5. The near wall temperature profile over the ribbed section was shifted upward compared with smooth surface, which indicated an increasing of the thermal layer.
6. The reduction of the viscous drag and Stanton number due the riblet was about (6 %) and (23 %) at Reynolds number range of$(1.5 \times 10^4 - 6 \times 10^4)$.

Nomenclature

Ch.	*Description*	*Units*
b	*Half duct height (H/2)*	*m*
C_p	*Specific heat at constant pressure*	*kJ/kg.K*
	skin friction coefficient	-

E	*the total energy of the fluid which is the sum of internal thermal energy and kinetic energy*	*kJ/kg*
H	*Duct height*	*m*
$\bar{h}$	*Average heat transfer coefficient*	*W/ m^2.K*
k	*Turbulent Kinetic Energy*	*m^2/s^2*
	Or Thermal conductivity	*W/m K*
	Riblet Spacing (Distance from Peak to Peak)	*m*
T	*Temperature*	*K*
	Friction Temperature	-
	The Non-Dimensional Temperature Difference.	-
	Friction velocity	*m/s*
	Local velocity normalized by Friction velocity $= u/u$	-
W	*Duct width*	*m*
X^*	*The distance from the beginning of test section in x-direction at x=311 cm*	*m*
u, v, w	*Time average Velocity Components*	*m/s*
x, y, z	*Cartesian Coordinates*	*m*

Greek Symbols

Ch.	**Description**	**Units**
	Diffusion Coefficient of Parameter	-
	Boundary layer thickness=b	m
	Dissipation Rate of Turbulent Kinetic Energy	m^2/s^2
	Heat transfer efficiency for ribbed surface	-
	Laminar (hydrodynamic) viscosity	$N.s/m^2$
	Density of Air	kg/m^3
	Kinematics Viscosity	m^2/s
	averaged Viscous Shear Stress	N/ m^2

<u>Non – Dimensional Parameters</u>

Ch.	**Description**	**Units**
	Reynolds number based on and Dh	-
Nu	*Average Nusselt Number*	-
Pr	*Prandtl number*	-

St	*Average Stanton Number*	-

Subscripts

a	*Air*	-
atm	*Atmospheric*	-
b	*Bulk value*	-
amb	*Ambient Temperature*	
bm	*Mean Bulk temperature between two locations*	-
con	*Heat transferred by conduction through the air between the upper and lower surface*	-
conv	*Heat transferred by forced convection*	
r	*Ribbed section*	-
sm	*Smooth section*	-
t	*Turbulent*	-
i,j	*Tenser form*	-
w	*Wall*	-

REFERENCES

[1]Chen J. J.,Leung Y. , andNorman W. M. KO.," Drag Reduction in a Longitudinally Grooved Flow Channel", Ind. Eng. Chem. Fundam., Vol. 25, No. 4,pp 741-745, 1986.

[2]Djenidi L., and Antonia R.A."A Turbulent Low Reynolds Number k-ε Model For Riblet Flow",11th Australasian Fluid mechanics Conference, University of Tasania, Hobart, Australia,14-18 December,1992.

[3]Choi K.-S., and Orchard D. M., "Turbulence Management Using Riblets for Heat and Momentum Transfer", Department of Mechanical Engineering ,University of Nottingham, Nottingham, United kgdom ,Experimental Thermal and Fluid Science, Vol. 15,pp 109-124,1997.

[4]Lin K.N., Christodoulou C., and Joseph D.D. ,"Drag Reduction in pipes Lined with Riblets", Structure of Turbulence and Drag Reduction IUTAM symposium Zürich /Switzerland ,pp. 545-551,1989.

[5]Benhalilou M.,and Kasagit N. ,"Numerical Prediction of Heat and Momentum Transfer over Micro-Grooved Surface with a Nonlinear k-ε Model ",International Journal of Heat and Mass Transfer,Vol.42,pp 1414-1430,1999.

[6]Stalio E., and Nobile E., "Direct Numerical Simulation of Heat Transfer over Riblets" , Dipartimento di Ingegneria Navale, del Mare e per l'Ambiente—Sezione di Fisica Tecnica, Universit._a di Trieste, Italy, International Journal of Heat and Fluid Flow ,Vol. 24,pp 356–371, 2003.

[7]Horsten B.J.C ,"A Numerical Study on Laminar and Turbulent Flow over Sharp and Blunt Sawtooth Riblets", viscous drag reduction mechanisms reviewed Delft university of technology ,Faculty of Aerospace Engineering ,August 26, 2005.

[8]Shaw R.,"Influence of Hole Dimensions on Static Pressure Measurements", J. Fluid Mechanics, Vol. 7, pp 550-564,1960. Pressure Measurements, www.chell.co.uk/psi/p-8400.htm.

[9]Oronzio M., Sergio N., and Daniele R., "Numerical Study of Air Forced Convection in a Channel Provided with Inclined Ribs" , Frontiers in Heat and Mass Transfer (FHMT), 2, 013007 ,2011.

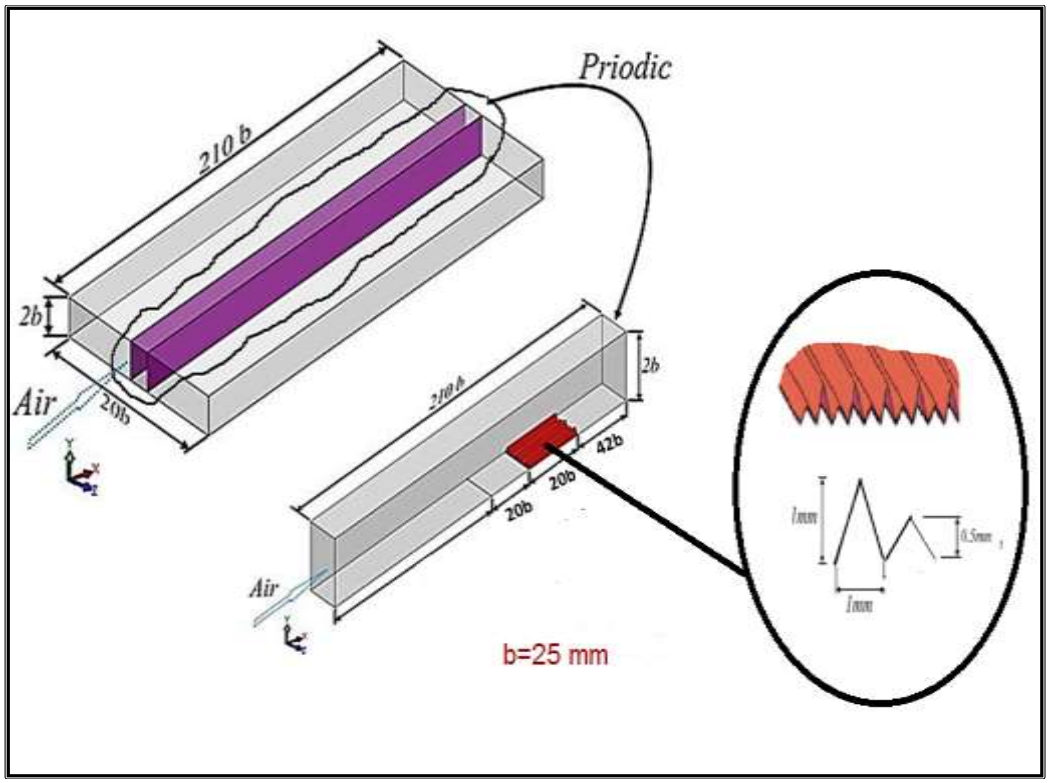

Figure. (1): The computation domain dimensions

Figure. (2): The Ribs dimensions and boundary condition.

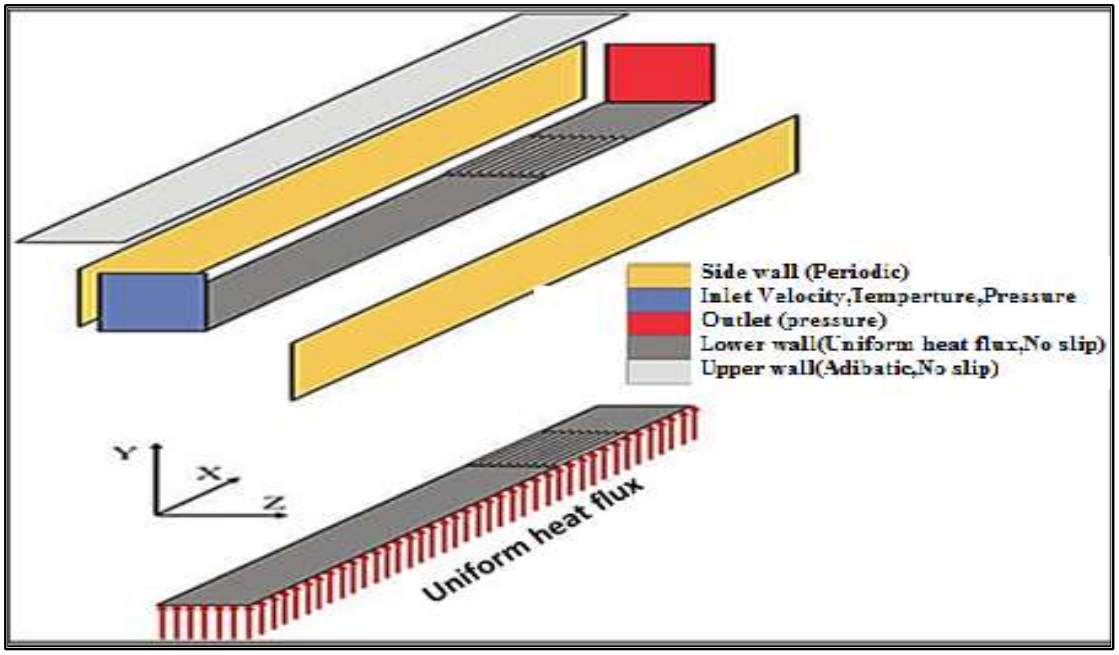

Figure. (3): The schematic diagram of experiment set up

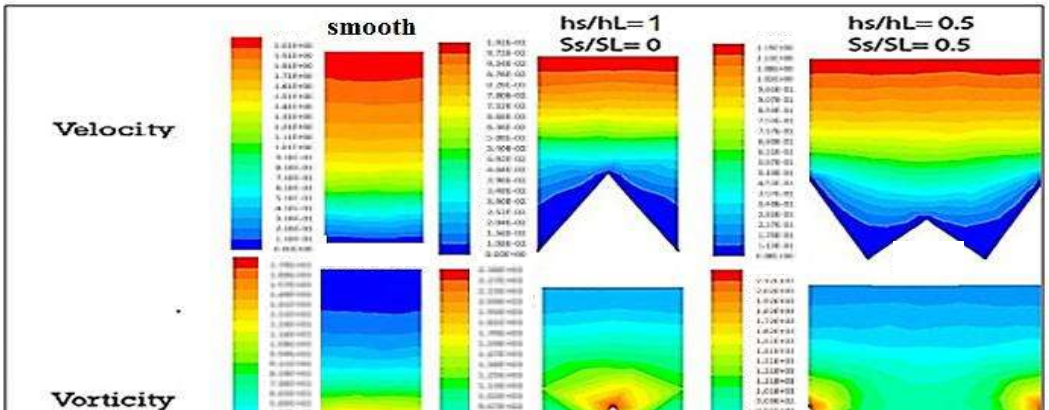

Figure.(4):Velocity,vorticity and secondary flow counters at mid plane of ribbed and smooth surface for two height ratios (1 and 0.5) at t Reynolds number

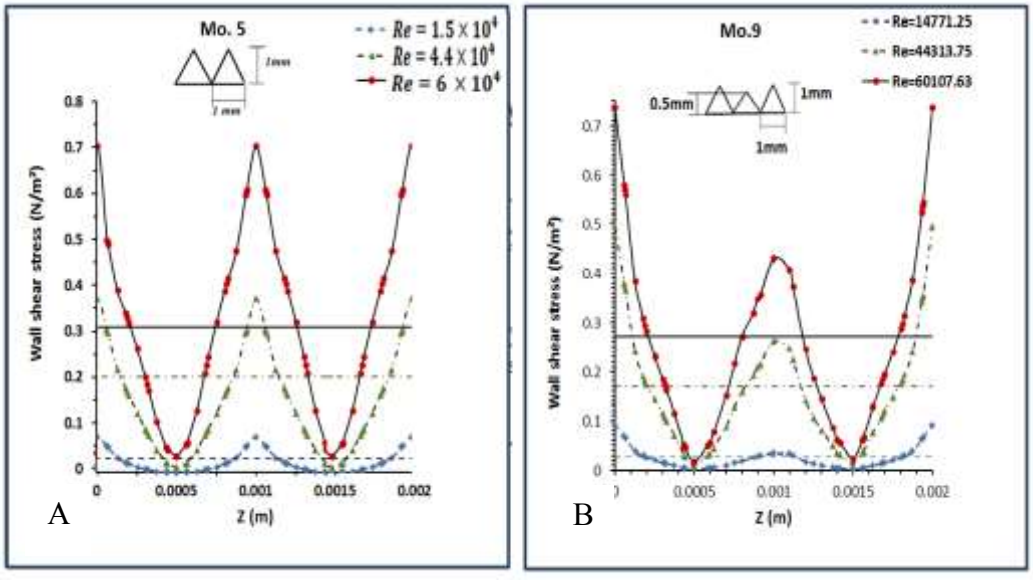

Figure. (5 A,B) :Local Wall Shear Stress distribution for two models [height ratios (1 and 0.5 respectively)] compared to smooth surface at three different Reynolds number.

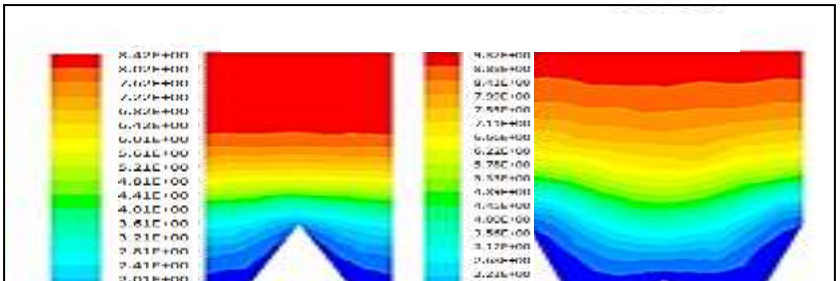

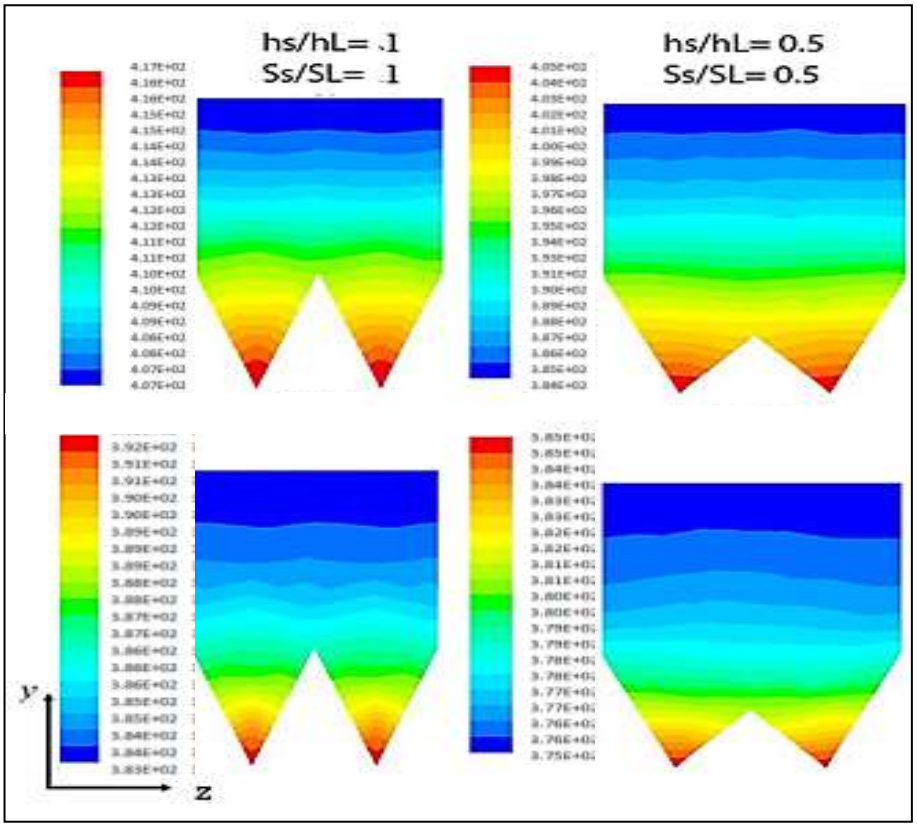

Figure. (7): Temperature magnitude (K) counters at mid plane of ribbed surface for two height ratios (1 and 0.5) at Reynolds number1

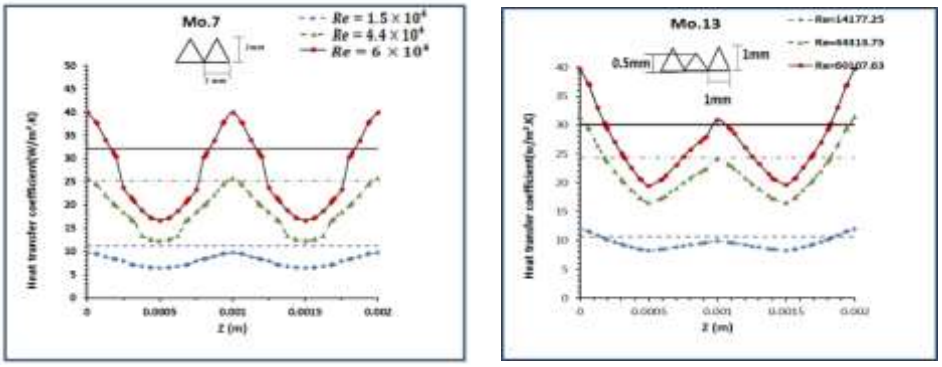

Figure. (8 A, B) local: Heat transfer coefficient distribution for two models [height ratios (1 and 0.5 respectively)] compared to smooth surface at three different Reynolds number.

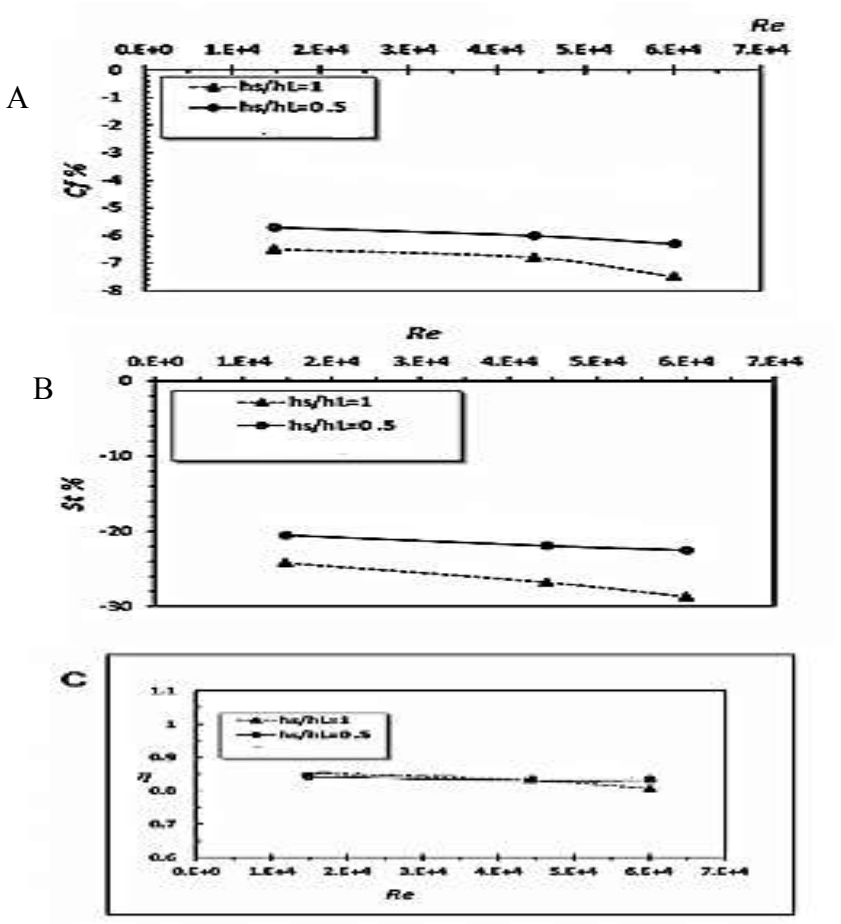

Figure. (9 A, B, C): Effect of change peak to peak height riblet in spanwise direction on flow and heat transfer characteristic of duct at rang of Reynolds number (1.5x104-6 x104)

A – Reduction of skin frictionC ———

B – Reduction of Stanton number ———

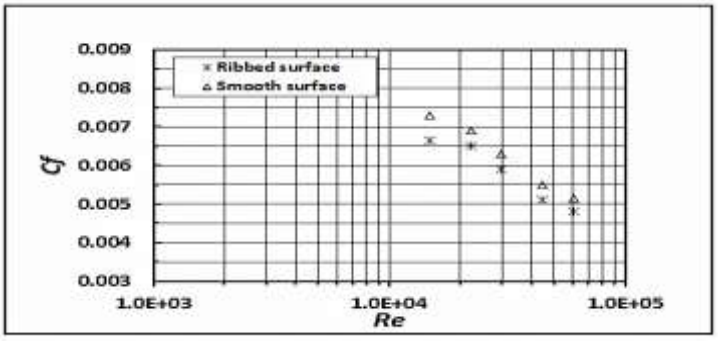

Figure (10): Experimental average skin friction coefficient for Smooth surface and ribbed surface for Reynolds range of(1.

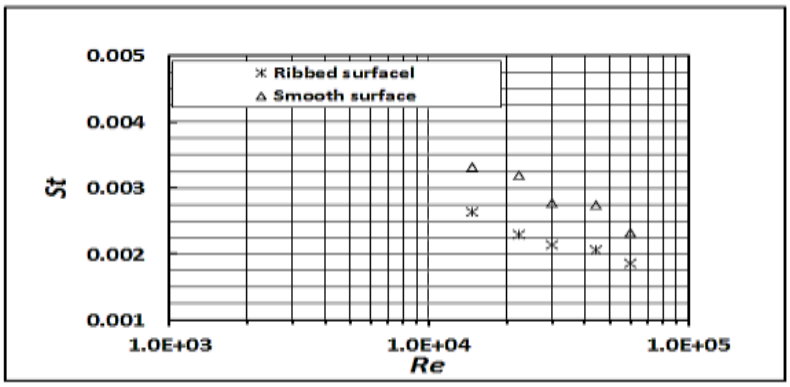

Figure. (11) Experimental average Stanton number For Smooth surface and ribbed surface For Revnolds range of(1.

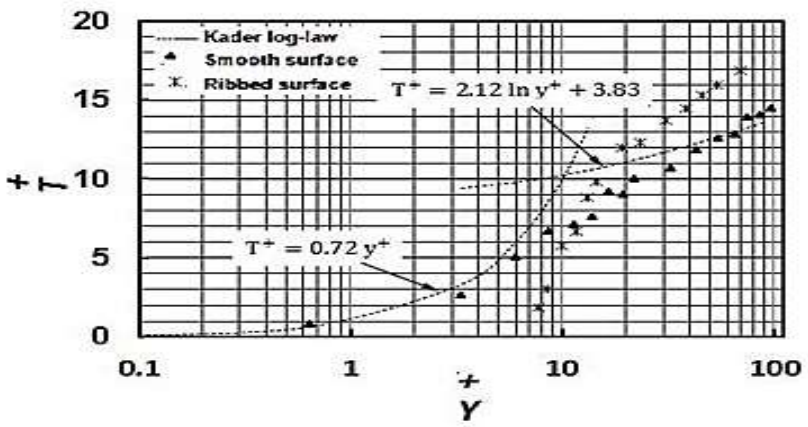

Figure. (12): Experimental near wall velocity profile at mid of the smooth surface (x*/b=10) and mid of ribbed surface (x*/b =30) (over rib tip) at $Re = 1.5 \times 10^4$.

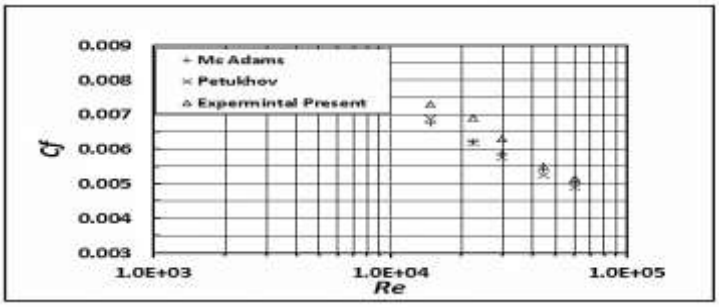

Figure (13): The comparison present experimental average skin friction coefficient for smooth surface with previous correlation at Reynolds number range of$(1.5 \times 10^4 - 6 \times 10^4)$.

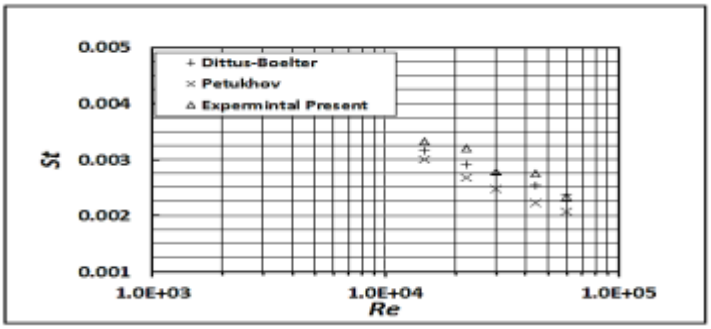

Figure (14): The comparison present experimental average Stanton number for smooth surface with previous correlation at Reynolds number range of($1.5 \times 10^4 - 6 \times 10^4$).

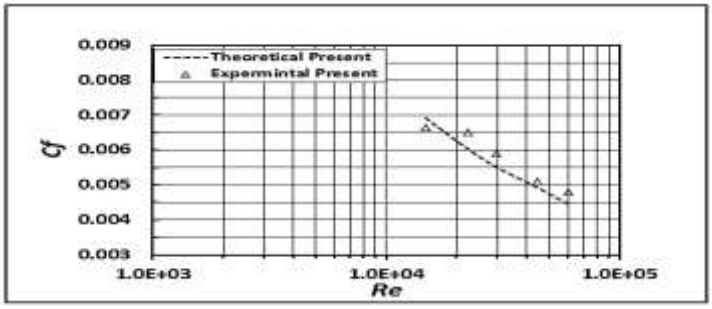

Figure. (15): The comparison of average skin friction coefficient between theoretical and experimental work for ribbed surface at Reynolds number range of($1.5 \times 10^4 - 6 \times 10^4$).

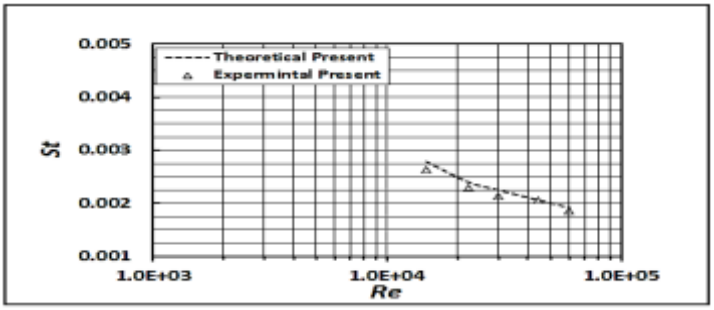

Figure. (16): The comparison of average Stanton Number between theoretical and experimental work for ribbed surface at Reynolds number range of).